Electronic Energy-Band Structure of SnS_2 and $SnSe_2$

C. Y. Fong
Department of Physics, University of California, Davis, California 95616

and

Marvin L. Cohen*
Department of Physics, University of California, Berkeley, California 94720
and Inorganic Material Research Division, Lawrence Radiation Laboratory, Berkeley, California 94720
(Received 6 July 1971)

The local-empirical-pseudopotential method is used to calculate the electronic band structure of SnS_2 and $SnSe_2$. The pseudopotential form factors for the constituent elements Sn, S, and Se are determined from previous pseudopotential calculations for other crystals. Slight adjustments were made to give the correct fundamental gaps. A group-theoretical study of the symmetry properties of these crystals is included. The imaginary part of the dielectric function, $\epsilon_2(\omega)$, is calculated for SnS_2. Some comparison is made between the theory and the existing experimental data.

I. INTRODUCTION

Compounds with layer structure show a wide range of electronic properties—from insulator to metal.[1] We concentrate here on two semiconducting tin chalcogenides, SnS_2 and $SnSe_2$. The semiconducting characteristics of $SnSe_2$ was predicted by Mooser and Pearson.[2] This prediction was verified experimentally by Busch *et al.*[3] and Asanabe[4] from conductivity, Hall effect, and thermoelectric measurements. The first reflectivity data was reported by Greenway and Nitsche[5] in the range 0.05 – 12.0 eV with polarization perpendicular to the $\vec{c}$ axis of the SnS_2 crystal. Their results give a shoulder at 3.8 eV and other structure at 4.9, 5.8, 6.9, and 7.6 eV. The indirect fundamental-optical-absorption edges were found to be at 2.07 and 0.97 eV for SnS_2 and $SnSe_2$, respectively, by Domingo *et al.*[6] These authors also found forbidden direct gaps at 2.88 eV for SnS_2 and at 1.63 eV for $SnSe_2$. Recently, Lee and Said[7] measured the absorption coefficient for $SnSe_2$ and determined the energy of the indirect gap to be 1.03 eV.

The first energy-band calculations for SnS_2 and $SnSe_2$ were reported by Au-Yang and Cohen.[8] Their results have several errors. The group theory was done incorrectly resulting in errors both in the symmetry assignments and in the calculated band structures. This work supersedes Ref. 8. In the present work the band structures were calculated using methods similar to Ref. 8. Because the most reliable experimental data relate only to the fundamental energy gaps, we determine the pseudopotential form factors by making small adjustments in the form factors extracted from other known pseudopotential calculations to give the experimental values for the band gaps. The paper is arranged as follows: In Sec. II, we give a group-theoretical analysis for the crystals. The method of calculation, the results, and comparisons with the experimental data are discussed in Sec. III.

II. GROUP-THEORETICAL ANALYSIS

The crystals SnS_2 and $SnSe_2$ crystallize in the CdI_2 type structure. The Bravais lattice of the structure is hexagonal. There is one molecule, e.g., CdI_2, per primitive cell. If one chooses the origin of the cell at the Cd atom, then the coordinates of the two I atoms are given by $\pm\vec{u}$, where $\vec{u} = (\frac{1}{3}a, \frac{2}{3}a, \frac{1}{4}c)$. The first two components in $\vec{u}$ are along two vectors $\vec{a}$ and $\vec{b}$ in the x-y plane placed 120° apart (Fig. 1), and the third component is along

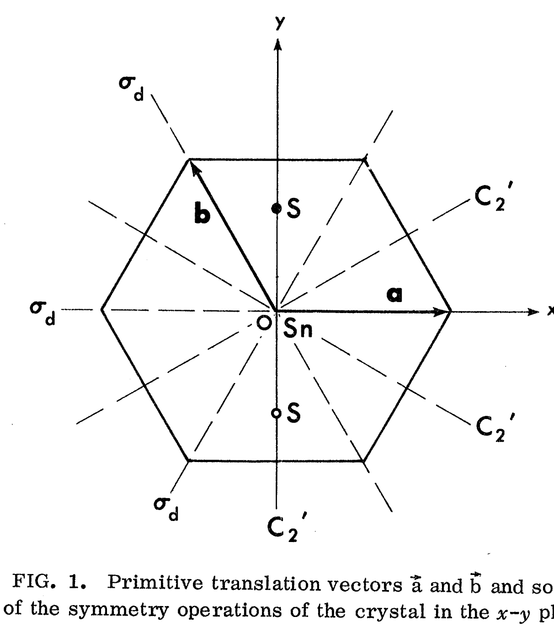

FIG. 1. Primitive translation vectors $\vec{a}$ and $\vec{b}$ and some of the symmetry operations of the crystal in the x-y plane.

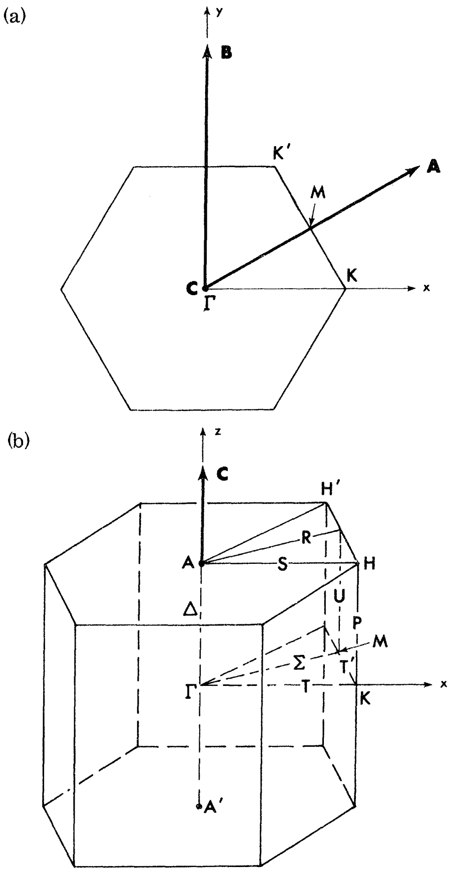

FIG. 2. (a) Two shortest reciprocal-lattice vectors $\vec{A}$ and $\vec{B}$ in the x-y plane. (b) First Brillouin zone for CdI_2 structure.

the vector $\vec{c}$ in the $\hat{z}$ direction. a and c are the usual lattice constants for the hexagonal structure.

The point group associated with CdI_2 structure is D_{3d}.[9] There are 12 symmetry operations which leave the crystal invariant. They are the identity operator E, two threefold rotations ($2C_3$) about the $\vec{c}$ axis, three twofold rotations ($3C_2'$) about the axes in the x-y plane and perpendicular to the sides of the hexagon (Fig. 1), the inversion operator i, two threefold rotations about the $\vec{c}$ axis followed by an inversion ($2iC_3$), and three twofold rotations followed by an inversion ($3iC_2'$). The last three operations are equivalent to $3\sigma_d$, the reflection in a "diagonal" plane[10] (Fig. 1).

The first Brillouin zone (BZ) of the hexagonal unit cell is also a hexagonal prism which is shown in Fig. 2(b). The two shortest reciprocal-lattice vectors $\vec{A}$ and $\vec{B}$ in the x-y plane determined from $\vec{a}$, $\vec{b}$, and $\vec{c}$ are shown in Fig. 2(a). The small groups associated with symmetry points and symmetry lines of the BZ are discussed as follows: The group at Γ is obviously D_{3d}. One can easily show that A has the same symmetry properties at Γ. For example, in Fig. 2(b), $\overrightarrow{\Gamma A}$ is transformed to $\overrightarrow{\Gamma A'}$ under inversion. However, the difference between $\overrightarrow{\Gamma A}$ and $\overrightarrow{\Gamma A'}$ is $\overrightarrow{AA'}$ which is a reciprocal-lattice vector with length $2\pi/c$; $\overrightarrow{\Gamma A}$ and $\overrightarrow{\Gamma A'}$ are therefore equivalent. The symmetry operators associated with M and L are the identity operator E; a two-fold rotation, C_2, about an axis, containing $\overrightarrow{\Gamma M}$; a reflection, σ_h, about plane containing $\overrightarrow{\Gamma A}$ and perpendicular to $\overrightarrow{\Gamma M}$; and the inversion operator, i. The group associated with these two points is C_{2h}.[11] Points K and H have the same symmetry operators as Γ and A except for the operators involving i, the inversion operator. They are associated with the group D_3. Vectors along the lines Σ, R, and U are invariant under E and σ_h defined for points M and L. These two operators form a group C_{1h}. The group associated with vectors along Δ is C_{3v}. Finally, T' and S' belong to C_2. A summary of the groups for various symmetry points and symmetry lines is listed in Table I. The character tables for two important small groups at $\Gamma(A)$ and $M(L)$ and the compatibility relations are given in Table II.

To study the optical properties of these two crystals, one has to measure the spectra by polarizing the incident light along and perpendicular to the $\vec{c}$ axis. The selection rules for the optical transitions are calculated for these two different polarizations. We give our results in Table III.

III. CALCULATIONS AND RESULTS

The method of calculation has been described elsewhere.[8] We just give a few important expressions to define the form factors.

The local-pseudopotential Hamiltonian neglecting spin-orbit interaction has the form

$$H = -(\hbar^2/2m)\nabla^2 + V(\vec{r}) \; . \quad (1)$$

The weak pseudopotential $V(\vec{r})$ is expanded in the reciprocal lattice

$$V(\vec{r}) = \sum_{\vec{G}} V(\vec{G})\, e^{i\vec{G}\cdot\vec{r}} \; , \quad (2)$$

$$V(\vec{G}) = \frac{1}{\Omega_{\text{cell}}} \int_{\text{cell}} V(\vec{r})\, e^{-\vec{G}\cdot\vec{r}}\, d^3r$$

$$= \frac{1}{\Omega_{\text{cell}}} \left[\Omega_{\text{Sn}} V^{\text{Sn}}(\vec{G}) + 2\Omega_{\text{S}} V^{\text{S}}(\vec{G}) \cos(\vec{G}\cdot\vec{u}) \right] , \quad (3)$$

TABLE I. Small groups associated with various symmetry points and symmetry lines in the Brillouin zone.

Symmetry points and lines	$\Gamma, A,$	K, H	Δ	M, L	Σ, R, U	T', S'
Group	D_{3d}	D_3	C_{3v}	C_{2h}	C_{1h}	C_2

TABLE II. Character tables for groups D_{3d} and C_{2h}, and compatibility relations for various symmetry points in the Brillouin zone.

	D_{3d}	E	$2C_3$	$3C_2'$	i	$2iC_3$	$3iC_2'=3\sigma_d$
	Γ_1	1	1	1	1	1	1
	Γ_2	1	1	−1	1	1	−1
	Γ_3	2	−1	0	2	−1	0
	$\Gamma_{1'}$	1	1	1	−1	−1	−1
z	$\Gamma_{2'}$	1	1	−1	−1	−1	1
x, y	$\Gamma_{3'}$	2	−1	0	−2	1	0

	C_{2h}	E	C_2	σ_h	i
	M_1	1	1	1	1
y	$M_{1'}$	1	1	−1	−1
	M_2	1	−1	−1	1
x, z	$M_{2'}$	1	−1	1	−1

$\Gamma(A)$			
$\Gamma_1(A_1)$	Δ_1	$\Sigma_1(R_1)$	$T_1(S_1)$
$\Gamma_2(A_2)$	Δ_2	$\Sigma_2(R_2)$	$T_2(S_2)$
$\Gamma_{1'}(A_{1'})$	Δ_2	$\Sigma_2(R_2)$	$T_1(S_1)$
$\Gamma_{2'}(A_{2'})$	Δ_1	$\Sigma_1(R_1)$	$T_2(S_2)$
$\Gamma_3, \Gamma_{3'}(A_3, A_{3'})$	Δ_3	$\Sigma_1+\Sigma_2(R_1+R_2)$	$T_1+T_2(S_1+S_2)$
$M(L)$			
$M_1(L_1)$	U_1	$\Sigma_1(R_1)$	$T_1'(S_1')$
$M_{1'}(L_{1'})$	U_2	$\Sigma_2(R_2)$	$T_1'(S_1')$
$M_2(L_2)$	U_2	$\Sigma_2(R_2)$	$T_2'(S_2')$
$M_{2'}(L_{2'})$	U_1	$\Sigma_1(R_1)$	$T_2'(S_2')$
$K(H)$			
$K_1(H_1)$	P_1	$T_1\ (S_1)$	$T_1'(S_1')$
$K_2(H_2)$	P_1	$T_2(S_2)$	$T_2'(S_2')$
$K_3(H_3)$	P_3	$T_1+T_2(S_1+S_2)$	$T_1'+T_2'(S_1'+S_2')$

where Ω_{cell} is the unit-cell volume of the crystal under consideration. Ω_{Sn} and Ω_S are volumes per atom in SnS_2. We truncate the expansion in $\vec{G}$ at

TABLE III. Selection rules for allowed transitions.

Perpendicular polarizations

$\Gamma_1(A_1) \leftrightarrow \Gamma_{3'}(A_{3'})$, $\Gamma_3(A_3) \leftrightarrow \Gamma_{1'}(A_{1'})$, $\Gamma_{2'}(A_{2'}) \leftrightarrow \Gamma_3(A_3)$,
$\Gamma_3(A_3) \leftrightarrow \Gamma_{3'}(A_{3'})$, $\Gamma_2(A_2) \leftrightarrow \Gamma_{3'}(A_{3'})$.
$M_1(L_1) \leftrightarrow M_{2'}(L_{2'})$ and $M_{1'}(L_{1'})$,
$M_2(L_2) \leftrightarrow M_{1'}(L_{1'})$ and $M_{2'}(L_{2'})$.
$\Delta_1 \leftrightarrow \Delta_3$, $\Delta_3 \leftrightarrow \Delta_3$, $\Delta_2 \leftrightarrow \Delta_3$.
$P_1 \leftrightarrow P_3$.
$K_1(H_1) \leftrightarrow K_3(H_3)$, $K_3(H_3) \leftrightarrow K_3(H_3)$, $K_2(H_2) \leftrightarrow K_3(H_3)$.
$\Sigma_1(U_1) \leftrightarrow \Sigma_1(U_1)$, $\Sigma_2(U_2) \leftrightarrow \Sigma_2(U_2)$, $\Sigma_1(U_1) \leftrightarrow \Sigma_2(U_2)$.

Parallel polarizations

$\Gamma_1(A_1) \leftrightarrow \Gamma_{2'}(A_{2'})$, $\Gamma_{1'}(A_{1'}) \leftrightarrow \Gamma_2(A_2)$, $\Gamma_3(A_3) \leftrightarrow \Gamma_{3'}(A_{3'})$.
$M_1(L_1) \leftrightarrow M_{2'}(L_{2'})$, $M_2(L_2) \leftrightarrow M_{1'}(L_{1'})$.
$\Delta_1 \leftrightarrow \Delta_1$, $\Delta_3 \leftrightarrow \Delta_3$, $\Delta_2 \leftrightarrow \Delta_2$.
$P_1 \leftrightarrow P_1$, $P_3 \leftrightarrow P_3$.
$K_1(H_1) \leftrightarrow K_2(H_2)$, $K_3(H_3) \leftrightarrow K_3(H_3)$.
$\Sigma_1(U_1) \leftrightarrow \Sigma_1(U_1)$, $\Sigma_2(U_2) \leftrightarrow \Sigma_2(U_2)$.

$|\vec{G}_{max}|^2 = \frac{59}{4}(2\pi/a)^2$. This limits the expansion to 16 nonvanishing pseudopotential form factors for Sn and 15 for S. Equation (1) is then solved by expanding the periodic part of the Bloch state in plane waves. The cutoff energies as defined in Ref. 12 are $E_1 = 9.1$ and $E_2 = 25.1$, which give the convergence of energy gaps at Γ, M, and L to the order of 0.1 eV. The size of the matrix is about 55×55. There are roughly 190 plane waves contributing to the Löwdin perturbation scheme as modified by Brust.[13] Because of the fact that the best known data for these two compounds are the forbidden indirect and direct energy gaps, we simply adjust (slightly) the scaled potentials of Sn, S, and Se from other calculations as discussed in Ref. 8 to fit these experimental data. The comparison of the resulting elemental pseudopotential form factors from the present calculations and the extracted ones from other calculations are shown in Fig. 3. The form factors are normalized to the following volumes: 67.50 Å^3 for Sn and S; and 76.67 Å^3 for Se. The pseudopotential form factors are given in Table IV. The $|\vec{G}|^2$'s are in units of $(2\pi/a_{ZB})^2$, where $a_{ZB} = \sqrt{2}a$ and ZB refers to the zinc blende structure. We use the form factors obtained by Animalu and Heine[14] for Sn, because their results give the form factors at large $|\vec{G}|$. For S and Se, we compare the results of present calculations with the results obtained by Cohen and Bergstresser[12] (CB) and Walter and Cohen[15] (WC).

The symmetry properties of crystals of the CdI_2 structure allow us to diagonalize the pseudopotential Hamiltonian on a mesh which is $\frac{1}{12}$ of the Brillouin zone. The total number of points in the mesh is 225. The band structure along symmetry

TABLE IV. Pseudopotential form factors in Ry.

	SnS_2		$SnSe_2$	
$\vec{G}$	V_{Sn}[a] (Ry)	V_S (Ry)	V_{Sn} (Ry)	V_{Se} (Ry)
(001)	−0.117		−0.0985	
(100)	−0.0362	−0.126	−0.048	−0.125
(002)	−0.0208	−0.0987	−0.0386	−0.086
(101)	−0.0185	−0.081	−0.0358	−0.071
(102)	0.0181	−0.0237	0.0096	−0.0338
(003)	0.0247	−0.0088	0.0173	−0.0098
(210)	0.0322	0.0019	0.0222	0.0018
(211)	0.0318	0.0091	0.0222	0.0098
(103)	0.0294	0.0146	0.0251	0.0124
(200)	0.0273	0.019	0.0236	0.0153
(212)	0.0265	0.0205	0.0236	0.0167
(201)	0.0261	0.0217	0.0229	0.0178
(004)	0.0241	0.0225	0.0214	0.0178
(202)	0.0193	0.0201	0.0185	0.015
(104)	0.0145	0.0158	0.0159	0.0132
(213)	0.0145	0.0158	0.0159	0.0132

[a]All V's normalized to the respective unit hexagonal cell volume.

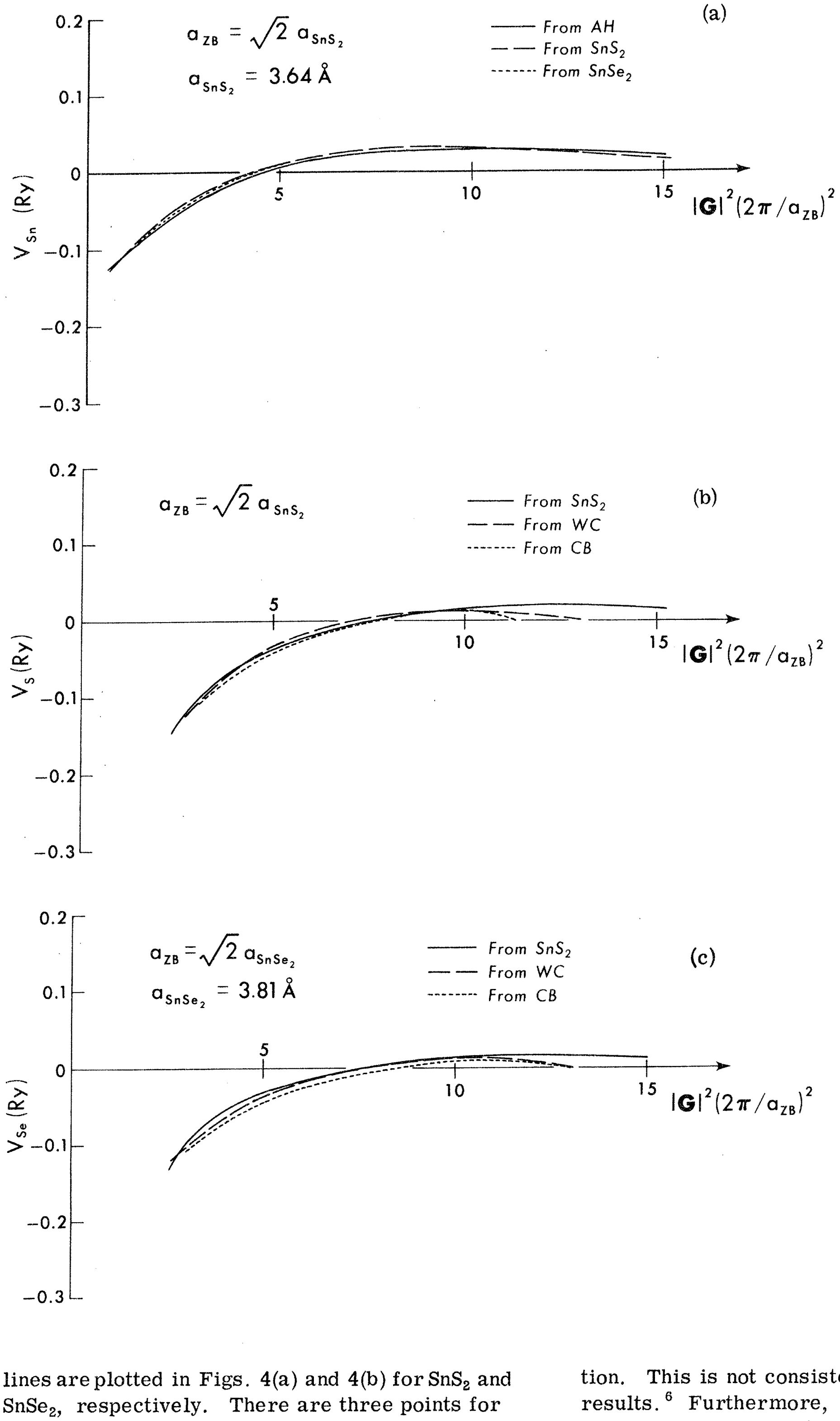

FIG. 3. (a) Comparison of pseudopotential form factors for Sn. AH is Ref. 14. (b) Comparison of pseudopotential form factors for S. WC and CB are Refs. 15 and 12, respectively. (c) Comparison of pseudopotential form factors for Se.

lines are plotted in Figs. 4(a) and 4(b) for SnS_2 and $SnSe_2$, respectively. There are three points for SnS_2 along U such that the lowest conduction-band energies are 0.2 eV less than the corresponding value at L. If this were the case, then the indirect fundamental transition would be an allowed transition. This is not consistent with the experimental results.[6] Furthermore, it is very difficult to push the lowest conduction band up along U by changing the form factors. We use a technique discussed by Cahn and Cohen[16] to calculate the lowest conduction-band energy at these points by using $m^* = 0.98$

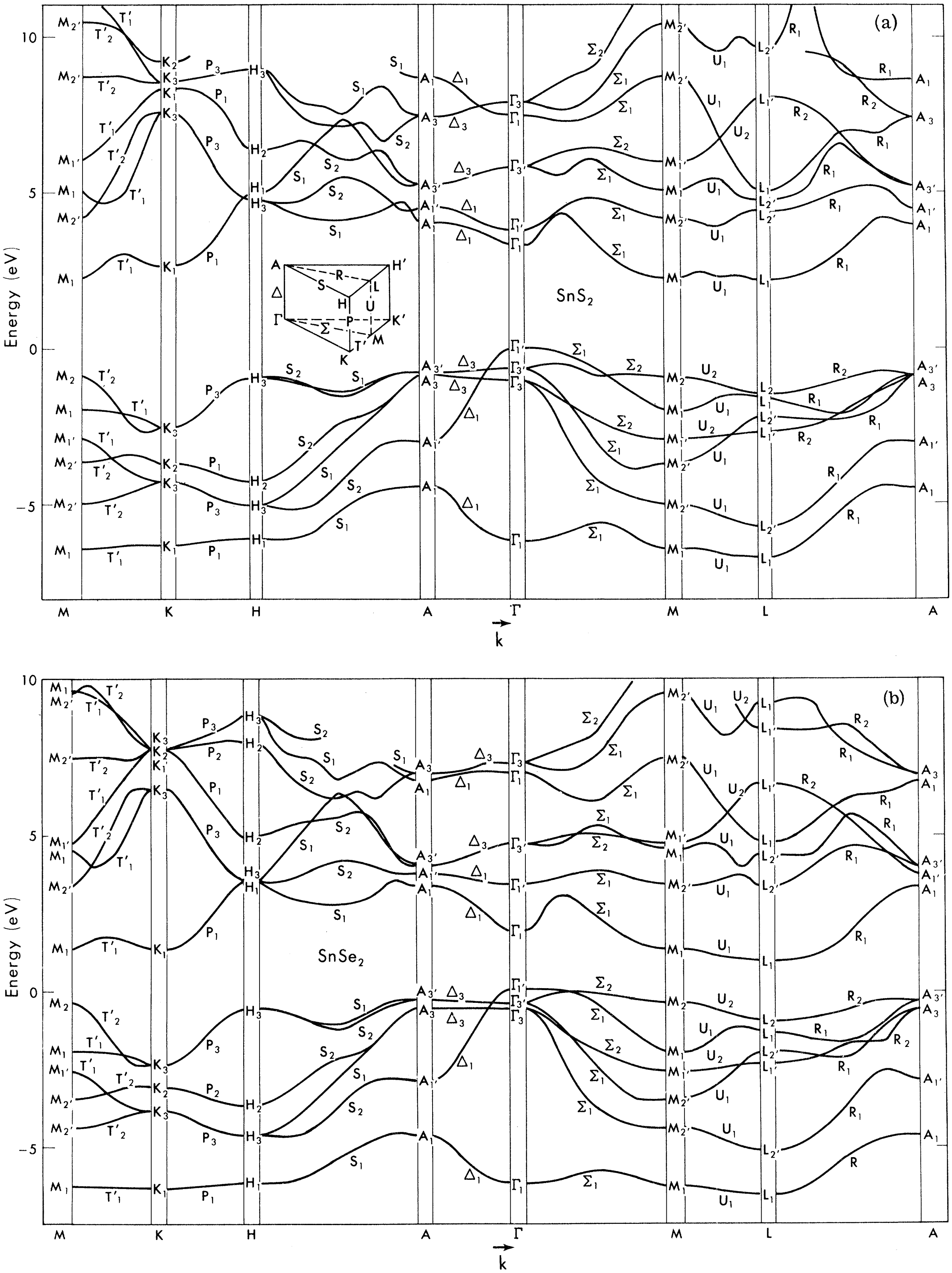

FIG. 4. (a) Band structure of SnS_2. (b) Band structure of $SnSe_2$; the second and third conduction bands along A to L become close in energy near A, but do not cross.

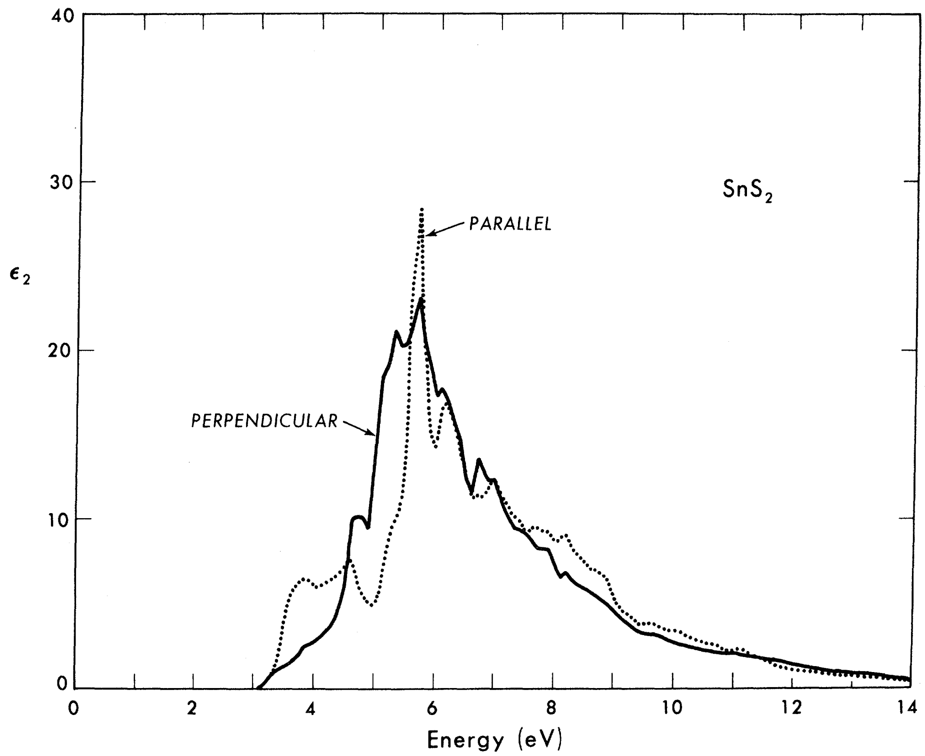

FIG. 5. Calculated $\epsilon_2(\omega)$ for SnS_2.

m. In $SnSe_2$, there are two points which cause the same difficulty. It is resolved by the same method.

These band-structure calculations are considered to be preliminary because of a lack of sufficient experimental data, especially for $SnSe_2$. Therefore, we calculate the $\epsilon_2(\omega)$, the imaginary part of the dielectric function, for SnS_2 only. Using the results of the energy-band-structure calculation, we evaluate $\epsilon_2(\omega)$ by

$$\epsilon_{2\parallel}(\omega)=\frac{4\pi^2e^2\hbar}{m^2\omega^2}\sum_{\vec{k}}\sum_{c,v}|\langle u_{c,\vec{k}}|\nabla_\parallel|u_{v,\vec{k}}\rangle|^2\delta(\omega_{cv}-\omega)\ , \tag{4}$$

$$\epsilon_{2\perp}(\omega)=\frac{4\pi^2e^2\hbar}{2m^2\omega^2}\sum_{\vec{k}}\sum_{c,v}|\langle u_{c,\vec{k}}|\nabla_\perp|u_{v,\vec{k}}\rangle|^2\delta(\omega_{cv}-\omega)\ , \tag{5}$$

where $\epsilon_{2\parallel}$ and $\epsilon_{2\perp}$ are $\epsilon_2(\omega)$ with light polarized parallel and perpendicular to the $\vec{c}$ axis. $u_{c,\vec{k}}$ and $u_{v,\vec{k}}$ denote the periodic part of the conduction-band and valence-band pseudo-wave-functions at $\vec{k}$. $\nabla_\parallel$ and $\nabla_\perp$ are the gradient operators parallel and perpendicular to the $\vec{c}$ axis. $\hbar\omega_{cv}$ is the energy gap between the conduction band and the valence band. The results for $\epsilon_{2\parallel}(\omega)$ and $\epsilon_{2\perp}(\omega)$ are plotted in Fig. 5.

The fundamental gap is indirect and forbidden for both compounds. The experimental values[6] are 2.07 and 0.97 eV for SnS_2 and $SnSe_2$, respectively; the corresponding values from the calculations are 2.19 and 0.91 eV. Both these transitions are from Γ to L, and are forbidden transitions. The calculated lowest direct energy gaps for SnS_2 and $SnSe_2$ are 3.15 and 1.75 eV. They occur at M and are forbidden by parity. The forbidden direct gaps measured by Domingo *et al.*[6] are 2.88 (SnS_2) and 1.62 eV ($SnSe_2$). The theoretical and experimental results for the lowest-energy gaps therefore agree quite well. A summary is given in Table V. The structures in $\epsilon_{2\perp}(\omega)$ occur at 3.9, 4.8, 5.4, 5.8, and 6.8 eV. They correlate quite well with

TABLE V. Summary of fundamental energy gaps for SnS_2 and $SnSe_2$.

Optical transitions	Material	Ref. 6 (expt.) (eV)	Ref. 7 (eV)	This work (eV)
Forbidden indirect transitions	SnS_2	2.07		2.19 ($\Gamma_{1'}\rightarrow L_1$)
	$SnSe_2$	0.97	1.03	0.91 ($\Gamma_{1'}\rightarrow L_1$)
Forbidden direct transitions	SnS_2	2.88		3.15 ($M_2\rightarrow M_1$)
	$SnSe_2$	1.62		1.75 ($M_2\rightarrow M_1$)

TABLE VI. Summary of main structure in the calculated $\epsilon_{2\perp}(\omega)$ for SnS_2 and the measured reflectivity.

Structure in reflectivity (eV)	Structure in $\epsilon_{2\perp}(\omega)$ (eV)	Identification main transitions
3.8	3.9	$M_0\ \Gamma_{3'} \rightarrow \Gamma_1$
	4.0	Volume effect $7\rightarrow 9$, $8\rightarrow 9$
4.9	4.9	Volume effect $6\rightarrow 9$, $7\rightarrow 9$, $8\rightarrow 9$
	5.4	$6\rightarrow 9$, $7\rightarrow 9$, $7\rightarrow 10$, $8\rightarrow 10$
5.8	5.7	$6\rightarrow 9$, $7\rightarrow 9$, $7\rightarrow 10$, $8\rightarrow 10$
6.9	6.8	$6\rightarrow 10$, $7\rightarrow 10$, $8\rightarrow 10$, $7\rightarrow 11$, $8\rightarrow 11$

the experimental reflectivity[5] curve with structure at 3.8, 4.9, 5.8, and 6.9 eV. There is no experimental optical data for SnS_2 with light polarized along the $\vec{c}$ axis. We summarize the structure in $\epsilon_2(\omega)$ and the measured reflectivity in Table VI.

ACKNOWLEDGMENTS

We would like to thank Professor L. M. Falicov for helpful discussions. One of us (M. L. C.) would like to thank Dr. M. Y. Au-Yang, Dr. W. Saslow, Dr. P. B. Allen, and Dr. P. B. Murray for their comments. We would also like to express our appreciation to Dr. P. B. Murray for his valuable criticism of the final manuscript. Part of this work was done under the auspices of the U. S. Atomic Energy Commission.

*Work supported in part by the National Science Foundation under Grant No. 13632.

[1]See for example, J. A. Wilson and A. D. Yoffe, Advan. Phys. 18, 193 (1969).

[2]E. Mooser and W. B. Pearson, Phys. Rev. 101, 492 (1956).

[3]G. Busch, C. Frohlich, and F. Hulliger, Helv. Phys. Acta 34, 359 (1961).

[4]S. Asanabe, J. Phys. Soc. Japan 16, 1789 (1961).

[5]D. L. Greenway and R. Nitsche, J. Phys. Chem. Solids 26, 1445 (1965).

[6]G. Domingo, R. S. Itoga, and C. R. Kannewurf, Phys. Rev. 143, 536 (1966).

[7]P. A. Lee and G. Said, J. Phys. 1, 837 (1968).

[8]M. Y. Au-Yang and M. L. Cohen, Phys. Rev. 178, 1279 (1969).

[9]R. W. G. Wyckoff, *Crystal Structure*, 2nd ed. (Interscience, New York, 1963), p. 266.

[10]M. Tinkham, *Group Theory and Quantum Mechanics* (McGraw-Hill, New York, 1964), p. 53.

[11]See, for example, A. W. Luehrmann, Ph.D. thesis (University of Chicago, 1967) (unpublished).

[12]M. L. Cohen and T. K. Bergstresser, Phys. Rev. 141, 789 (1966).

[13]D. Brust, Phys. Rev. 134, A1337 (1964).

[14]A. O. E. Aminalu and V. Heine, Phil. Mag. 12, 1249 (1965).

[15]J. P. Walter and M. L. Cohen, Phys. Rev. 183, 763 (1969).

[16]R. N. Cahn and M. L. Cohen, Phys. Rev. B 1, 2569 (1970).

PHYSICAL REVIEW B VOLUME 5, NUMBER 8 15 APRIL 1972

Frequency- and Wave-Vector-Dependent Dielectric Function for Silicon†

John P. Walter* and Marvin L. Cohen

Department of Physics, University of California and Inorganic Materials Research Division, Lawrence Radiation Laboratory, Berkeley, California 94720

(Received 15 November 1971)

The frequency- and wave-vector-dependent complex dielectric function $\epsilon(\vec{q}, \omega)$ is calculated for silicon. The energy eigenvalues and eigenvectors which are used have been obtained from energy-band calculations based on the empirical pseudopotential method. Explicit results are given in the [100] direction in the range $0 \leq q \leq (2\pi/a)$ and $0 \leq \hbar\omega \leq 24$ eV. A comparison is made between the present results and the results of a calculation of $\epsilon(q, \omega)$ for a free-electron gas in the random-phase approximation.

I. INTRODUCTION

We have calculated the frequency- and wave-vector-dependent dielectric function $\epsilon(\vec{q}, \omega)$ in the [100] direction for silicon. This is the first calculation of $\epsilon(\vec{q}, \omega)$ for a semiconductor in which realistic energy eigenvalues and eigenvectors are used. Previous calculations of dielectric functions have concentrated either on the wave-vector-dependent dielectric function[1] for zero frequency $\epsilon(\vec{q}, \omega=0)$ or on the frequency-dependent dielectric function[2] $\epsilon(\vec{q}=0, \omega)$. The former case is important in determining the static screening of electric fields, and the latter case is important in analyzing the optical properties of semiconductors because q is approximately zero for optical wave vectors. The more general dielectric function $\epsilon(\vec{q}, \omega)$ describes the screening of a longitudinal field which